

# Photoinduced Volume Transition in Liquid Crystalline Polymer Gels Swollen by a Nematic Solvent

Yuki Hayata,<sup>†,‡</sup> Shusaku Nagano,<sup>§,||</sup> Yukikazu Takeoka,<sup>†</sup> and Takahiro Seki<sup>\*,†</sup>

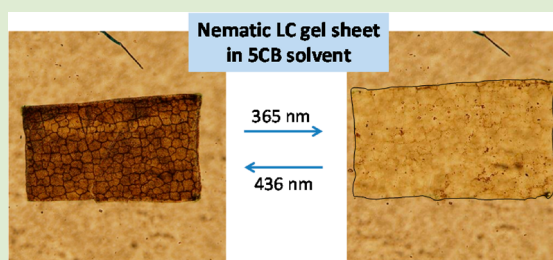
<sup>†</sup>Department of Molecular Design and Engineering, Graduate School of Engineering, Nagoya University, Furo-cho, Chikusa, Nagoya 464-8603, Japan

<sup>§</sup>Nagoya University Venture Business Laboratory, Furo-cho, Chikusa, Nagoya 464-8603, Japan

<sup>||</sup>PRESTO, Japan Science and Technology Agency, Tokyo 102-0076, Japan

## S Supporting Information

**ABSTRACT:** Nematic liquid crystalline (LC) cross-linked polymer gel sheets containing 3 mol % azobenzene (Az) unit were prepared and swollen by a nematic solvent of 4'-pentyl-4-cyanobiphenyl (5CB). This 5CB-swollen gel sheet exhibited a discontinuous volume change around the nematic-isotropic phase transition temperature of the LC gel ( $T_{NI}^G$ ). UV irradiation at a temperature slightly lower than  $T_{NI}^G$  provoked a large volume transition (expansion) due to a loss of nematic order within the gel sheet caused by the trans-to-cis photoisomerization of Az. The volume was reverted by irradiation with 436 nm light. By templating the colloidal crystal film of monodispersed silica particles, a LC gel sheet possessing a microporous structure was also prepared. Due to the facilitated diffusion of 5CB, the microporous LC gel exhibited significant enhancements in the extent and rate of the photoinduced volume transition.



Stimuli-induced volume changes and transitions in solvent-swollen cross-linked polymer gels have long been the subject of great interest from fundamental polymer physics to applications for actuators, micromechanics and artificial muscles.<sup>1,2</sup> Among them, solvent-swollen liquid crystalline (LC) gels have unique properties in that the alignment of mesogenic groups and their orientational order at the molecular level are directly coupled with the macroscopic volume and shape changes. Theoretical studies have suggested that orientational (nematic) ordering effect can induce a volume transition of gels. A mean field theory shows that a gel with nematic liquid crystallinity immersed in isotropic or nematic solvents exhibits a volume transition triggered by orientational ordering inside the gel.<sup>3–5</sup> Experimentally, such theoretical predictions are confirmed systematically by Urayama et al.<sup>6–10</sup> Depending on the nematic order inside and outside of the gel network, the gel absorbs or expels the isotropic or nematic solvent, resulting in a considerable volume changes and deformations of the cross-linked gel material. The change in the orientational order and phase transition can be controlled by temperature change<sup>6–8</sup> or application of external electric field.<sup>8–11</sup>

On the other hand, photoinduced macroscopic dynamic deformations of molecular crystals<sup>12–15</sup> and LC polymer materials<sup>16–27</sup> have become a great stream of research in recent years. Such materials are expected to provide future elements of smart actuators, microrobots, micropumps, sensors, and so on that work in noncontact and addressable manners. In most cases, photochromic molecules and polymers are

employed, and the shape changes and deformations undergo in reversible manners. To date, all these photomechanical effects are achieved in solid condensed states. To our knowledge, despite the above efforts, the photomechanical macroscopic motions based on the light-triggered change of the orientational order in “open” solvent-swollen LC gel systems have not been examined so far.

We show herein that the photochemically modulated molecular ordering and disordering in LC gels are able to cause significant volume transitions. The volume transition is accompanied by a solvent flow driven by the chemical potential change coupled with the molecular orientational order. For this purpose, embedding azobenzene (Az) groups into the LC gel would be most promising.<sup>28–30</sup> The photoinduced order change is provoked by the trans-to-cis and cis-to-trans photoisomerization of Az groups inducing a large change in the molecular structure from a mesogenic rodlike shape of the *trans*-isomer to a bend nonmesogenic shape of the *cis*-isomer.

The compounds and abbreviations used in this study are shown in Figure 1. For the requirement of uniform light irradiation, the gel sample was prepared as a sheet. A mixture of CB6Ac, 5Az6Ac, HDAc (cross-linker), and a photoinitiator prepared at a molar ratio of 92:3:3:2 was sandwiched between a cell of two glass plates (6  $\mu\text{m}$  gap adjusted by silica particles) and subjected to photoinitiated free radical polymerization at

**Received:** August 31, 2012

**Accepted:** November 5, 2012

**Published:** November 8, 2012

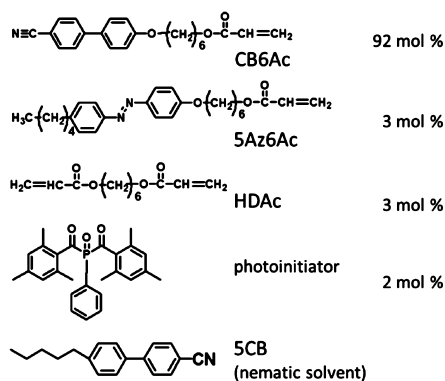


Figure 1. Chemical structures of compounds used in this study.

100 °C for 30 min. A polydomain LC polymer sheet obtained as above was then removed from the glass cell and immersed in 5CB. The thermal analysis and polarized optical microscopic (POM) observations reveal that the nematic–isotropic transition temperatures of pure 5CB ( $T_{NI}^S$ ) and the 5CB-swollen LC gel with 5CB ( $T_{NI}^G$ ) were 35 and 51 °C, respectively (Figures 1S and 2S in Supporting Information).

Figure 2 shows the equilibrium swelling degree of the gel sheet ( $Q = A/A_0$ ,  $A$  and  $A_0$  being the sheet areas in swollen in

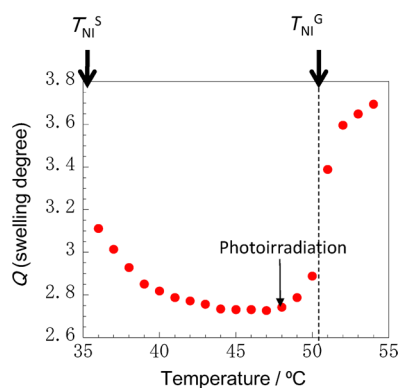


Figure 2. Equilibrium swelling degree  $Q$  vs temperature. The temperature for the photoinduced volume changes (48 °C) is also indicated.

5CB and dry states, respectively) as a function of temperature ranging 36–54 °C. Here, the swelling of the gel sheet was evaluated as the area increase because the real time estimation of the thickness change was difficult. With increasing temperature starting from 36 °C,  $Q$  was reduced continuously and exhibited a sudden increase around 51 °C corresponding to  $T_{NI}^G$ . This profile qualitatively agrees well with the volume changes reported by Urayama et al.<sup>6–8</sup> and accord with the predictions of the mean-field theory for nematic gel.<sup>3–5</sup> It was therefore anticipated that UV light irradiation to the gel sheet at an appropriate temperature (a temperature slightly lower than  $T_{NI}^G$ ) will be able to induce photochemically the nematic to isotropic phase transition.

The UV–visible absorption spectral changes of the gel sheet are displayed in Figures 3a and 3b. The typical reversible photochromic behavior of Az was observed in the spectral changes at the  $\pi$ – $\pi^*$  (around 370 nm) and  $n$ – $\pi^*$  (around 450 nm) absorption bands. The spectral change indicates that the photoisomerization undergoes highly efficiently as in solutions. We introduced 3 mol % of the Az unit in the gel sheet and this

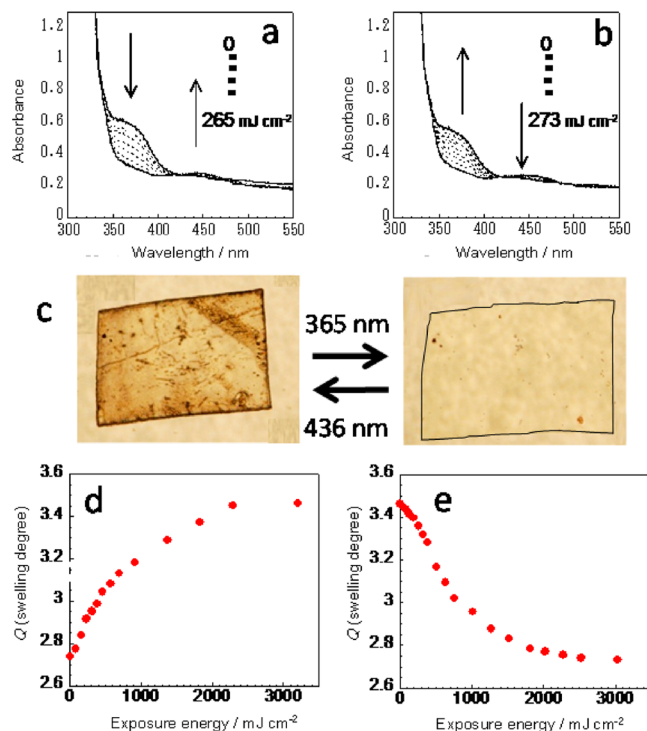


Figure 3. (a) UV–visible absorption spectral changes of a 5CB-swollen LC gel sheet upon 365 nm light irradiation at 40 °C starting from the *trans*-Az state (this temperature was chosen to minimize the turbidity change). (b) UV–visible absorption spectral changes upon 436 nm light irradiation at 40 °C starting from the final state of (a). (c) Microscopic images of a LC gel sheet upon alternate 365 and 436 nm light irradiation. The initial size of the LC gel sheet before immersion into 5CB was about 1 × 1.5 mm. (d) Area expansion profile during 365 nm light irradiation (7.6 mW cm<sup>-2</sup>). (e) Area contraction profile during 436 nm light irradiation (5.0 mW cm<sup>-2</sup>).

condition was appropriate for all Az units within the gel to undergo the photoisomerization.

Upon UV (365 nm) light irradiation at 48 °C, the gel sheet actually exhibited a significant expansion. The area expanded by 1.25-fold of the original in 420 s (3200 mJ cm<sup>-2</sup>). The gel sheet reverted to the original size upon visible light (436 nm) irradiation in 700 s (3000 mJ cm<sup>-2</sup>; Figure 3d,e and Movies 1 and 2 in Supporting Information). Figure 3c shows the optical microscopic photograph showing the reversible volume change of the gel sheet upon alternative UV and visible light irradiation at 48 °C. The degree of swelling and volume change were not as large as observed by Urayama et al.<sup>6</sup> This should be ascribed to the difference in the polymerization conditions. Their LC networks were polymerized in solution, and in our case, by contrast, the bulk polymerization without solvent was employed. To monitor the photoinduced phase transition, POM observation was achieved under UV irradiation. A multicolored birefringent character of the LC gel sheet was lost by irradiation (Supporting Information, Figure 3S), however, minor birefringency still remained. This fact should indicate the heterogeneity of the network structure. The photoinduced phase transition occurs in less constrained regions, whereas it is suppressed in more constrained ones. The initial multicolored LC gel sheet turned to a uniform white one by UV irradiation, indicating that the stubborn LC regions should be local in size.

In the mass open system, the extent and rate of volume change should be dependent on the diffusion of the solvent.

Therefore, introduction of a porous structure in the gel sheet was anticipated to improve the volume change properties.<sup>31</sup> Here, a colloidal crystal film consisting of monodispersed silica particles of 300 nm diameter was used for the template to prepare a microporous LC gel sheet. The silica colloidal crystal film was immersed into the identical LC monomer mixtures as mentioned above and subjected to the photopolymerization. After the polymerization, the composite film was immersed in hydrofluoric acid aqueous solution for one week to dissolve the silica. The details of the preparation procedures of colloidal crystal film are described in the Experimental Section. The scanning electron microscopic (SEM) images of the LC sheet after dissolving the silica particles taken from the top and cross section are indicated in Figures 4a,b, respectively. As shown, the

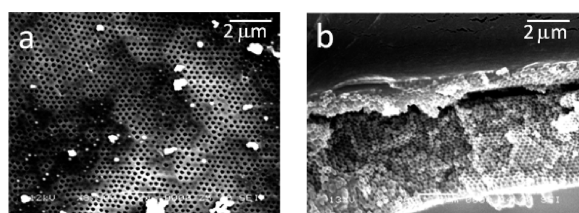


**Figure 4.** SEM images of a microporous LC gel sheet (a, top view; b, cross section).

LC film contains highly ordered hexagonally packed spherical micropores. The resulting microporous LC gel sheet swollen by SCB exhibited a greenish color. The peak top of the photonic band gap positioned at 502 nm.

The equilibrium  $Q$  values of the LC gel sheets with and without the micropores at varied temperatures are displayed in Figure 5a, and microscopic photos of the porous LC gel sheet

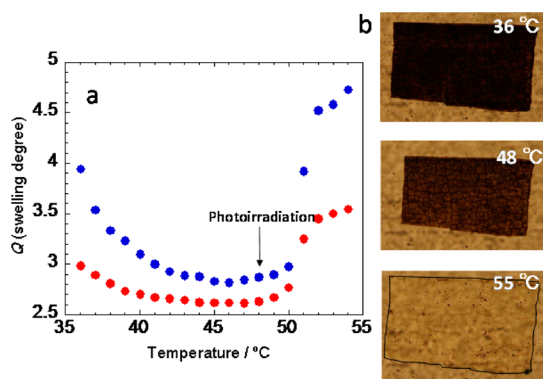


**Figure 5.** (a) Equilibrium swelling degree  $Q$  vs temperature. Blue and red circles denote the plots for SCB-swollen LC sheets with and without the microporous structure, respectively. (b) Optical microscopic images of a microporous gel sheet at temperatures indicated in the pictures. The initial size of the LC gel sheet before immersion into SCB was ca.  $1 \times 2$  mm.

at three typical temperatures in Figure 5b. The features of the profiles with temperature are essentially the same for the two systems, however, the swelling degree and volume changes around  $T_{NI}^G$  became obviously prominent by introduction of the microporous structure. The  $Q$  value at 54 °C become larger from 3.6 to 4.8 by introducing the micropores. It is likely that the LC gel sheet having the compartmented micropore structure are able to be deformed more readily at micrometer scales. The volume expansion around  $T_{NI}^G$  was further

enhanced. The ratio of  $Q(54 \text{ °C})/Q(48 \text{ °C})$  was 1.66 and 1.38 for the LC sheet with and without the porous structure, respectively. Figure 5b shows the color and the area changes at three given temperatures. The microporous gel film at lower temperatures (36 and 48 °C) looked dark in the microscope field, due to stronger light scattering, suggesting that structural heterogeneities are involved. Probably, the micropores are collapsed at the lower temperatures. The sheet became transparent above  $T_{NI}^G$  (55 °C) via swelling with SCB into both the LC gel network and micropores, providing a homogeneous (isotropic) refractive index within the gel sheet.

The photinduced volume transition also became prominent (Figure 6 and Movies 3 and 4 in Supporting

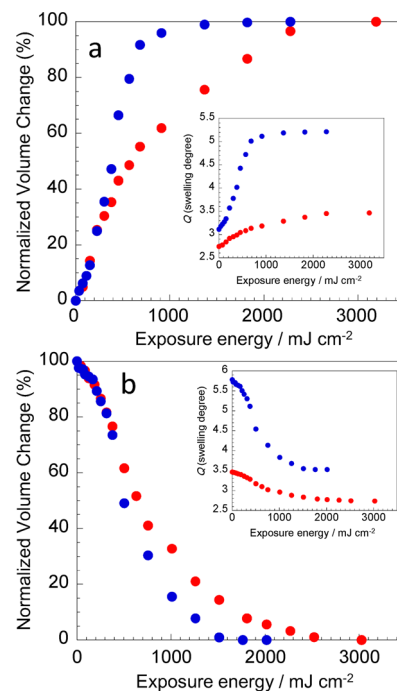


**Figure 6.** (a) Normalized volume changes (%) for the 365 nm light-induced volume expansion process. (b) The same profile for the 436 nm light-induced contraction process. In both plots, the inset depicts  $Q$  vs irradiation energy. In all figures, blue and red plots correspond to the gel sheet with and without the microporous structure. The thickness of the sheet was  $6 \mu\text{m}$  in both types of LC gel sheet. The light intensities are the same as indicated in Figure 3.

Information). The UV (365 nm) induced area increases estimated by a ratio of  $Q(\text{after UV})/Q(\text{before UV})$  at 48 °C were 1.25 and 1.70 for the nonporous and porous LC gel films, respectively (see inset of Figure 6a). The deformation rate can be compared with the profiles of the normalized  $Q$  versus the light energy of exposed. During the UV light irradiation, the expansion for the microporous gel sheet almost ceased around  $1000 \text{ mJ cm}^{-2}$ , which is approximately one-third of that for the LC gel sheet without micropores (Figure 6a). In the reversed process on 436 nm light irradiation, the shrinkage motion for the microporous LC gel was completed at  $1500 \text{ mJ cm}^{-2}$ , which is half of that required for the gel sheet without micropores. In this way, introduction of micropores in the gel significantly improves the volume transition properties due to the facilitated diffusion of the free solvent in the micropores.

In conclusion, this work proposes new light-driven motions driven by the nematic solvent-flow directly coupled with the

orientational order of the gel and solvent. Mass migrations based on the change in the nematic order can be found in other systems, for example, condensations of amorphous polymer chains<sup>32,33</sup> and nanoparticles<sup>34</sup> as impurities in nematic LC media. The impurities migrate to be condensed or aligned in less-ordered regions such as disclinations<sup>33,34</sup> and light-induced disordered spot<sup>32</sup> in nematic LC media. It is anticipated that manipulations of LC order by light or other means may find new practical applications with dynamic functions ranging from molecular to macroscopic levels.

## EXPERIMENTAL SECTION

Materials and synthesis of mesogenic acrylate monomers (CB6Ac and 5Az6Ac) were described in the Supporting Information. Light (436 nm) irradiation for the photopolymerization was achieved with a mercury–xenon lamp (Supercure 302S, San-ei Electronics) passing through an appropriate combination of optical filters.

Preparation of LC gel sheet containing microspores was performed as follows. The preparation of silica colloidal crystal films and the procedures for templated porous LC sheet was prepared according to the previous report.<sup>35</sup> A suspension of the monodispersed particles (300 nm, Nippon Shokubai Co. Ltd.) was diluted to a target concentration using deionized water. Then a cleaned hydrophilic glass substrate was immersed vertically into the dispersion and lifted up at a precisely controlled speed of  $0.04 \mu\text{m s}^{-1}$  using an ALV-104-HP lifter (Chuo Precision Industrial Co. Ltd.). The colloidal crystal film obtained as above was covered with another glass plate, and immersed into the identical mixture of LC monomers. The photopolymerization conditions are the same as those for the LC sheet without colloidal crystals. After polymerization, the two glass plates are removed and immersed into 10% (by weight) hydrofluoric aqueous solution at room temperature for one week. The film was then washed with pure water sufficiently. After drying, the porous film was immersed into SCB to obtain a LC gel.

Differential scanning calorimetry (DSC) and POM were performed with a Seiko Instruments DSC220 and an Olympus BX51, respectively. The UV visible absorption spectra were taken on an Agilent 8453. The reflection spectrum of the microporous LC gel was taken with a home-built apparatus arranging parts of Ocean Optics (light source: LS-1, spectrometer: USB-2000 vis-NIR and fiber scope: R-400–7-vis/R). The SEM observation was performed with a JSM-5600 (JEOL).

For the observation of area changes of the gel sheet was achieved using an Olympus BX51 microscope. The LC gel sheet was cut to a small piece of typically  $1 \times 1.5$  mm area with a razor blade. The temperature of the sheet was controlled with a Mettler-Torred FP-90. Each sample was kept at a given temperature for 2 h to establish the equilibrium. The area of the LC sheet was evaluated from the microscopic image using an image analysis software. The light irradiation to the LC gel sheet was performed with a mercury lamp light source equipped in the BX-51 microscope. The wavelength was selected using a set of optical filters. The light intensity was monitored by a TQ8210 Advantest optical power meter.

## ASSOCIATED CONTENT

### Supporting Information

Materials and synthetic procedures, DSC, POM data, and movies of the photoinduced volume changes. This material is available free of charge via the Internet at <http://pubs.acs.org>.

## AUTHOR INFORMATION

### Corresponding Author

\*E-mail: [tseki@apchem.nagoya-u.ac.jp](mailto:tseki@apchem.nagoya-u.ac.jp).

### Present Address

<sup>‡</sup>Toyota Motor Corporation, Toyota City, Aichi Prefecture 471-8571, Japan.

## Notes

The authors declare no competing financial interest.

## ACKNOWLEDGMENTS

The research was supported by the Grant-In-Aid for Basic Research S (to T.S., No. 23225003) from the Ministry of Education, Culture, Sports, Science and Technology, Japan, and PRESTO program of Japan Science and Technology Agency (to S.N.).

## REFERENCES

- (1) Tanaka, T. *Sci. Am.* **1981**, *244*, 124.
- (2) Yoshida, R.; Okano, T. Stimuli-Responsive Hydrogels and Their Application to Functional Materials. In *Biomedical Applications of Hydrogels Handbook*; Ottenbrite, R. M., et al. Eds.; Springer: Berlin/Heidelberg, 2010; pp 19–43.
- (3) Warner, M.; Wang, X.-J. *Macromolecules* **1992**, *25*, 445.
- (4) Matsuyama, A.; Kato, T. *Phys. Rev. E* **1999**, *59*, 763.
- (5) Matsuyama, A.; Kato, T. *J. Chem. Phys.* **2002**, *116*, 8175.
- (6) Urayama, K.; Okuno, Y.; Kawamura, T.; Kohjiya, S. *Macromolecules* **2002**, *35*, 4567.
- (7) Urayama, K.; Okubo, Y.; Nakano, T.; Takigawa, T. *J. Chem. Phys.* **2003**, *118*, 2903.
- (8) Urayama, K. *Macromolecules* **2007**, *40*, 2277.
- (9) Urayama, K.; Kondo, H.; Arai, Y. O.; Takigawa, T. *Phys. Rev. E* **2005**, *71*, 051713.
- (10) Fukunaga, A.; Urayama, K.; Koelsch, P.; Takigawa, T. *Phys. Rev. E* **2005**, *79*, 051702.
- (11) Kishi, R.; Suzuki, Y.; Ichujo, H.; Hirasa, O. *Chem. Lett.* **1994**, 2257.
- (12) Kobatake, S.; Takami, S.; Muto, H.; Ishikawa, T.; Irie, M. *Nature* **2007**, *446*, 778.
- (13) Terao, F.; Morimoto, M.; Irie, M. *Angew. Chem., Int. Ed.* **2012**, *51*, 901.
- (14) Koshima, H.; Ojima, N.; Uchimoto, H. *J. Am. Chem. Soc.* **2009**, *131*, 6890.
- (15) Uchida, K.; Sukata, A.; Matsuzawa, U.; Akazawa, M.; de Jong, J. D.; Katsonis, N.; Kojima, Y.; Nakamura, S.; Areephong, J.; Meetsma, A.; Feringa, B. L. *Chem. Commun.* **2008**, 326.
- (16) Finkelmann, H.; Nishikawa, E.; Pereira, G. G.; Warner, M. *Phys. Rev. Lett.* **2001**, *87*, 015501.
- (17) Li, M.-H.; Keller, P.; Ki, B.; Wang, X.; Brunet, M. *Adv. Mater.* **2003**, *15*, 569.
- (18) Ikeda, T.; Nakano, M.; Yu, Y.; Tsutsumi, O.; Kanazawa, A. *Adv. Mater.* **2003**, *15*, 201.
- (19) Barrett, C. J.; Mamiya, J.; Yager, K. G.; Ikeda, T. *Soft Matter* **2007**, *3*, 1249.
- (20) Yu, Y.; Nakano, M.; Ikeda, T. *Nature* **2003**, *425*, 145.
- (21) Ikeda, T.; Mamiya, J.; Yu, Y. *Angew. Chem., Int. Ed.* **2007**, *46*, 506.
- (22) Priimagi, A.; Shimamura, A.; Kondo, M.; Hiraoka, T.; Kubo, S.; Mamiya, J.; Konoshita, M.; Ikeda, T.; Shishido, A. *ACS Macro Lett.* **2011**, *1*, 96.
- (23) Harris, K. D.; Cuypers, R.; Scheibe, P.; van Oosten, C. L.; Bastiaansen, C. W. M.; Lub, J.; Broer, D. J. *J. Mater. Chem.* **2005**, *15*, 5043.
- (24) van Oosten, C. L.; Bastiaansen, C. W. M.; Broer, D. J. *Nat. Mater.* **2009**, *8*, 677.
- (25) Camacho-Lopez, M.; Finkelmann, H.; Palffy-Muhoray, P.; Shelly, M. *Nat. Mater.* **2004**, *3*, 307.
- (26) Wei, J.; Yu, Y. *Soft Matter* **2012**, *8*, 8050.
- (27) Hosono, N.; Kajitani, T.; Fukushima, T.; Ito, K.; Sasaki, S.; Takata, M.; Aida, T. *Science* **2010**, *330*, 808.
- (28) Ikeda, T. *J. Mater. Chem.* **2003**, *13*, 2037.
- (29) Yu, H.; Ikeda, T. *Adv. Mater.* **2011**, *23*, 2149.
- (30) Seki, T. *Bull. Chem. Soc. Jpn.* **2007**, *80*, 2084.
- (31) Takeoka, Y.; Watanabe, M. *Langmuir* **2002**, *18*, 5977.
- (32) Samitsu, S.; Takanishi, Y.; Yamamoto, J. *Nat. Mater.* **2010**, *9*, 816.

- (33) Kikuchi, H.; Yokota, M.; Hisakado, Y.; Yang, H.; Kajiyama, T. *Nat. Mater.* **2002**, *1*, 64.
- (34) Higashiguchi, K.; Yasui, K.; Ozawa, M.; Odoi, K.; Kikuchi, H. *Polym. J.* **2012**, *44*, 632.
- (35) Honda, M.; Seki, T.; Takeoka, Y. *Adv. Mater.* **2009**, *21*, 1801.